Journal of Magnetic Resonance 194 (2008) 58–66

Contents lists available at ScienceDirect

Journal of Magnetic Resonance

journal homepage: www.elsevier.com/locate/jmr

Exploring the limits of broadband excitation and inversion: II. Rf-power optimized pulses

Kyryl Kobzar [a], Thomas E. Skinner [b], Navin Khaneja [c], Steffen J. Glaser [a], Burkhard Luy [a,*]

[a] Institut für Organische Chemie und Biochemie, Technische Universität München, Lichtenbergstrasse 4, D-85747 Garching, Germany
[b] Physics Department, Wright State University, Dayton, OH 45435, USA
[c] Division of Engineering and Applied Sciences, Harvard University, 29 Oxford Street, Cambridge, MA 02138, USA

ARTICLE INFO

Article history:
Received 28 February 2008
Revised 27 May 2008
Available online 30 June 2008

Keywords:
Optimal control theory
Excitation
Inversion
Rf-power
BEBOP
BIBOP
Broadband pulses

ABSTRACT

In [K. Kobzar, T.E. Skinner, N. Khaneja, S.J. Glaser, B. Luy, Exploring the limits of broadband excitation and inversion, J. Magn. Reson. 170 (2004) 236–243], optimal control theory was employed in a systematic study to establish physical limits for the minimum rf-amplitudes required in broadband excitation and inversion pulses. In a number of cases, however, experimental schemes are not limited by rf-amplitudes, but by the overall rf-power applied to a sample. We therefore conducted a second systematic study of excitation and inversion pulses of varying pulse durations with respect to bandwidth and rf-tolerances, but this time using a modified algorithm involving restricted rf-power. The resulting pulses display a variety of pulse shapes with highly modulated rf-amplitudes and generally show better performance than corresponding pulses with identical pulse length and rf-power, but limited rf-amplitude. A detailed description of pulse shapes and their performance is given for the so-called power-BEBOP and power-BIBOP pulses.

1. Introduction

The development of broadband excitation and inversion pulses with tolerance to B_1-field inhomogeneity is a long-standing goal in NMR spectroscopy [1–20]. Usually, the performance of such pulses is limited by the available rf-amplitude. In a number of applications, however, the overall rf-power of an experiment proves to be the main restriction. Examples are heteronuclear decoupling schemes in high resolution NMR, where the applied rf-power can damage the probehead, or approaches in magnetic resonance imaging with strict FDA guidelines for rf-power deposition.

It is of both theoretical and experimental interest to know the physical limits of potential excitation and inversion pulses. We therefore studied systematically the performance of rf-amplitude-limited pulses with respect to pulse duration, bandwidth, and tolerance to rf-amplitude variations using algorithms based on optimal control theory [21].

The application of optimal control theory to the design of pulses [22–30] is well-established by now. It involves the calculation of a gradient towards better performing pulse parameters based on an analytical formula and allows the optimization of a very large number of independent parameters. In cases where the theoretical limits of quantum evolution are known [31–37], numerical algorithms based on principles of optimal control theory provide pulse sequences which approach the physical limits [38–40]. We therefore have reason to expect that BEBOP (broadband excitation by optimized pulses [25]) and BIBOP (broadband inversion by optimized pulses [21]) pulses perform close to the global optimum.

In this article, we present a systematic study of excitation and inversion pulses with unlimited rf-amplitude, but limited average rf-power. After introducing the algorithm, resulting pulse performances and pulse shapes are shown and compared to rf-amplitude-limited BEBOP/BIBOP and other published pulses.

2. Theory

Optimal control theory and its application to NMR spectroscopy is described in detail elsewhere [23–26,40]. The optimization algorithm used in the systematic studies of rf-power-limited excitation and inversion pulses presented in this article is very similar to the one used in [21,26] to limit the maximum rf-amplitude.

The quality factor or final cost Φ used in the optimizations is the transfer efficiency from the initial magnetization $\mathbf{M}(t_0) = \mathbf{M}_z$ to the target state $\mathbf{F}$ ($\mathbf{F} = \mathbf{M}_x$ for excitation and $\mathbf{F} = -\mathbf{M}_z$ for inversion pulses), averaged over all offsets and rf-amplitudes specified for a specific optimization. It can be written as

$$\Phi = \frac{1}{n_{\mathrm{off}} n_{\mathrm{rf}}} \sum_{i=1}^{n_{\mathrm{off}}} \sum_{j=1}^{n_{\mathrm{rf}}} \mathbf{M}_{ij}(t_{\mathrm{p}}) \cdot \mathbf{F} \qquad (1)$$

* Corresponding author. Fax: +49 89 289 13210.
E-mail address: burkhard.luy@ch.tum.de (B. Luy).

1090-7807/$ - see front matter © 2008 Elsevier Inc. All rights reserved.
doi:10.1016/j.jmr.2008.05.023

where $i = 1 \ldots n_{\text{off}}$ labels the various offset points and $j = 1 \ldots n_{\text{rf}}$ the scaled rf-amplitudes calculated for each pulse of length t_p, e.g. to include the effects of rf-inhomogeneity or rf-amplitude misadjustments. With the effective rf-field in the rotating frame ω_e given by

$$\begin{aligned}\omega_{\mathbf{e}} &= \omega_{\mathbf{1}}(\mathbf{t})[\cos\phi(\mathbf{t})\hat{\mathbf{x}} + \sin\phi(\mathbf{t})\hat{\mathbf{y}}] + \Delta\omega(\mathbf{t})\hat{\mathbf{z}} \\ &= \omega_{\text{rf}}(\mathbf{t}) + \Delta\omega(\mathbf{t})\hat{\mathbf{z}} \end{aligned} \quad (2)$$

the optimization procedure itself can be described by the following steps (see [25,26,40] for a more detailed derivation).

1. Choose an initial rf sequence $\omega_{\text{rf}}^{(0)}$.
2. Evolve $\mathbf{M}$ forward in time starting from $\mathbf{M}(t_0)$.
3. Calculate $\Gamma(t_p) = \mathbf{M}(t_p) \times \mathbf{F}$ for all offsets and scaled rf-amplitudes and evolve it backwards in time.
4. $\boldsymbol{\omega}_{\text{rf}}^{(k+1)}(t) \rightarrow \boldsymbol{\omega}_{\text{rf}}^{(k)}(t) + \epsilon \cdot \overline{\boldsymbol{\Gamma}(t)}$.
5. Calculate $\overline{P} = \frac{1}{t_p}\int_{t_0}^{t_p} \mathrm{d}t(\omega_1(t))^2$.
6. If $\overline{P} > P_{\max}$, set $\omega_1(t) \rightarrow \omega_1(t) \cdot \sqrt{\frac{P_{\max}}{\overline{P}}}$.
7. Repeat steps 2–6 until a desired convergence of Φ is reached.

$\overline{P}$ is proportional to the integral of the rf-power of the pulse, which in practice is calculated as the sum over all n piecewise constant segments of the shaped pulse $\overline{P} = \frac{1}{n}\sum_{m=1}^{n}(\omega_{1m}(t))^2$. The rf-power limit is typically given as the rf-amplitude of a corresponding constant amplitude pulse $\omega_{\max} = \sqrt{P_{\max}}$, which ensures direct comparability with previously optimized rf-amplitude-limited pulses [21]. Since the optimization is performed over a range of frequency offsets and variations in peak rf calibration, the gradient $\overline{\boldsymbol{\Gamma}}$ used in step 4 is averaged over the entire range. The incrementation ϵ is either chosen small enough to ensure convergence of the algorithm or it is determined by a linear minimization at each step. Instead of using directly the gradient $\overline{\boldsymbol{\Gamma}}$, we implemented its conjugated gradient in step 4 which results in even faster optimization convergence [40].

Using the described algorithm, the pulse performance was studied systematically in the following way. Sets of excitation and inversion pulses were calculated for bandwidths of 10, 20, 30, 40, and 50 kHz considering ideal rf-amplitude (no scaling factor applied). Also, sets of pulses for bandwidths of 10, 20, and 30 kHz with rf-amplitude variations of ϑ of ±10%, ±20%, ±30%, and ±40% (scaling factor applied on rf-amplitude is $1 + \vartheta$) were optimized to test robustness against B_1-field inhomogeneity. In all cases, the root mean square average rf-amplitude was limited to $\omega_{\max}$ = 10 kHz using the method described above.

For each set, pulse lengths t_p were varied in ranges as listed in Table 1. Generally, pulse durations were incremented until the quality factor Φ exceeded 0.995. Each chosen bandwidth was divided into equal increments, with n_{off} = 100. n_{rf} was chosen equal to 5 with equidistant percentage amplitude changes whenever variations in rf-amplitude were included in the calculations. The time digitization for the optimized shapes was 0.5 μs in all cases. One hundred randomized starting pulses were generated to start 100 optimizations for each data point in Figs. 1 and 2. As for pulses optimized with limited rf-amplitudes, the convergence of each single optimization was very fast, ranging from seconds for the shortest pulses to tens of minutes for the longer ones with larger n_{off} and n_{rf}. Computations were performed on several Linux-based PCs equipped with AMD Athlon processors.

3. Results

The results of the optimizations of excitation and inversion pulses are shown in Figs. 1 and 2, respectively. The performance of the optimized pulses described by the quality factor Φ is given as a function of pulse length on a linear scale in Figs. 1A, D and 2A, D. A logarithmic scale is used in Figs. 1B, E and 2B, E to show the differences at longer pulse durations more clearly. Figs. 1C, F and 2C, F show peak rf-amplitudes in corresponding pulses. As expected from our previous study, higher demands in terms of bandwidth or tolerance to rf-amplitude variation lead to reduced quality factors that can, however, be compensated by increased pulse lengths. The relation between duration and bandwidth is roughly linear for both types of pulses for the investigated offset and rf ranges.

Table 1
Constraints used for optimizations of pulses with limited average rf-power

$\Delta\nu$[a] (kHz)	ϑ[b] (%)	t_p excitation (μs)	t_p inversion (μs)
10	–	5–45	5–105
20	–	5–65	5–155
30	–	5–85	5–205
40	–	5–105	5–265
50	–	5–125	5–325
10	±10	5–95	5–135
10	±20	5–135	5–155
10	±30	5–185	5–195
10	±40	5–235	5–245
20	±10	5–125	5–175
20	±20	5–185	5–225
20	±30	5–255	5–295
20	±40	5–375	5–345
30	±10	5–175	5–255
30	±20	5–245	5–305
30	±30	5–345	5–325
30	±40	5–405	5–355

[a] $\Delta\nu$ is defined as the excitation/inversion bandwidth used in the optimization.
[b] ϑ corresponds to the range of rf-amplitude tolerance incorporated in the optimization.

In contrast to optimizations with limited rf-amplitude, a weak step or wave-like behavior of the cost Φ with respect to pulse duration is only observed for excitation pulses with significant tolerance to rf-inhomogeneity (c.f. Fig. 1D). The origin for these waves is unclear since no specific change in pulse families can be appointed to the steps. For excitation pulses with $\vartheta = 0$ and for inversion pulses, a very smooth, more or less exponential decrease of errors (defined as $1 - \Phi$) with respect to pulse duration can be observed for bandwidths of 20 kHz or larger. Indeed, the excitation pulses optimized with $\vartheta = 0$ all belong to the same pulse family, and all optimized inversion pulses belong to two pulse families that seem to be of equivalent quality.

The pulse shape of $\vartheta = 0$ excitation pulses is very similar to the phase-alternated ones shown in Fig. 3A–D with a sinc-like amplitude-modulation. The pulse shapes resemble to some extent polychromatic pulses and ICEBERG pulses for wideband excitation described in [18] and [41], which, however, were designed without constraints in power deposition. Interestingly, the maximum rf-amplitude of this class of pulses for a given performance increases roughly linearly with the desired bandwidth and is always reached at the end of the pulse shape. For the pulses with $\Phi > 0.995$ this maximum amplitude is, moreover, almost identical to the bandwidth. The same relation can be found for 90° hard pulses, where the phase-corrected excitation bandwidth with 99.5% transfer into the x, y-plane is about equal to their rf-amplitude (see e.g. Fig. 2B of [28]). For rf-power-limited excitation pulses optimized with respect to robustness against variations in rf-amplitude, in addition to the sinc-like pulse shapes, other shapes with more vivid amplitude and phase modulations appear (Fig. 3E). The vast majority of these pulse shapes shows an almost linear phase sweep on top of the fine modulations.

An inspection of pulse shapes produced for inversion pulses (c.f. Fig. 4) reveals that pulses of two families emerge: one family consists of constant phase, amplitude-modulated pulses that strongly

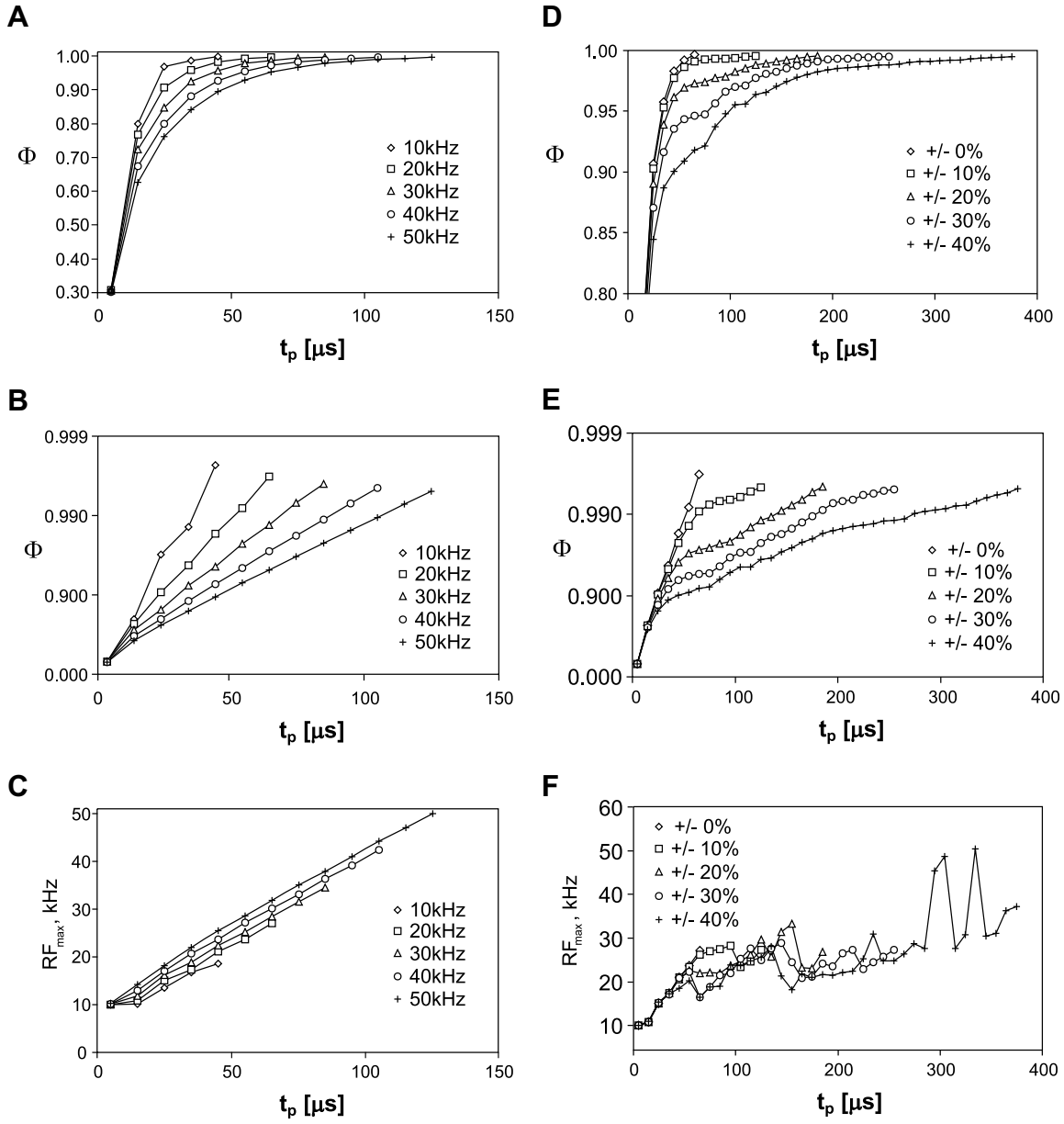

Fig. 1. Maximum quality factors reached for broadband excitation pulses with root mean square average rf-amplitude limited to 10 kHz under various optimization constraints. The maximum quality factor Φ with respect to pulse duration is given for the five different bandwidths $\Delta\nu$ equal to 10, 20, 30, 40, and 50 kHz on a linear (A) and logarithmic scale (B). In (C), the values of peak rf-amplitudes of corresponding pulses are plotted as a function of pulse length. The maximum quality factors Φ with respect to rf-variation are shown for rf-ranges ϑ of 0%, ±10%, ±20%, ±30%, and ±40% on a linear (D) and logarithmic scale (E) for a fixed bandwidth of 20 kHz. In (F), the values of peak rf-power of corresponding pulses are plotted as a function of pulse length.

resembles pulse shapes of known selective inversion pulses. The pulse shown in Fig. 4A, for example, looks very much like a Gaussian pulse [42] and the one of Fig. 4D is strikingly similar to a time-reversed G3 Gaussian-cascade pulse [43] or a selective time-reversed spline-based pulse [12]. The second pulse family shows a very smooth phase behavior similar to BIP [19] and BIBOP [21] pulses, but with an additional amplitude-modulation where the maximum rf-amplitude coincides with the central extremum of the phase (Fig. 4C and E). The shapes of the second family closely resemble the pulse shape derived in [44] for optimized decoupling at low rf-power levels with essentially identical requirements. For pulse lengths exceeding approximately 100 μs, both pulse families appear to be optimal in a random manner, suggesting that there are only minor differences in performance, if at all.

The limitation of the root mean square average rf-amplitude to 10 kHz in the presented study makes the results directly comparable to the ones obtained in [21] with limited rf-amplitude. A comparison of the performance curves for the two types of pulses in Figs. 5 and 6 clearly shows the overall better quality of the rf-power-limited pulses. The improvement is strongest for large bandwidth excitation without variation in rf-amplitude (5B), where up to two times shorter pulses lead to the identical pulse performance, and decreases with the introduction of B_1-variations (6). Apparently the overall improved performance is connected with the larger maximum rf-amplitude available in rf-power-limited pulses. While a distinct step or wave-like behavior is observed for the amplitude-limited pulses, the performance curves of power-limited pulses are very smooth as mentioned above.

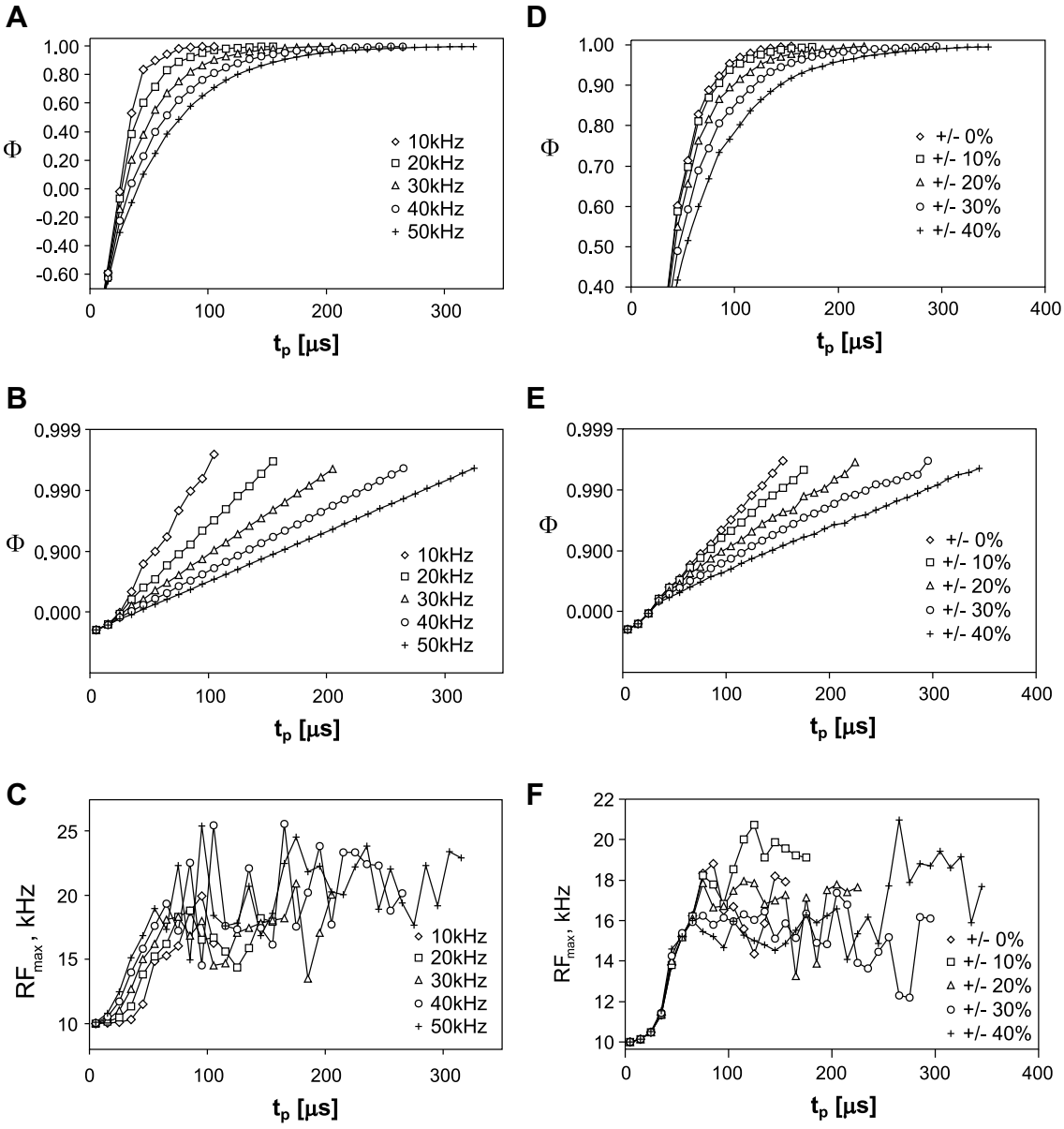

Fig. 2. Maximum quality factors reached for broadband inversion pulses with root mean square average rf-amplitude $\omega_{max} = \sqrt{P_{max}}$ limited to 10 kHz under various optimization constraints. The maximum quality factor Φ with respect to pulse duration is given for the five different bandwidths $\Delta\nu$ equal to 10, 20, 30, 40, and 50 kHz on a linear (A) and logarithmic scale (B). In (C), the values of peak rf-amplitude of corresponding pulses are plotted as a function of pulse length. The maximum quality factors Φ with respect to rf-variation are shown for rf-ranges ϑ of 0%, ±10%, ±20%, ±30%, and ±40% on a linear (D) and logarithmic scale (E) for a fixed bandwidth of 20 kHz. In (F), the values of peak rf-power of corresponding pulses are plotted as a function of pulse length.

As in [21], we calculated the quality factor Φ for a number of already published excitation and inversion pulses for comparison. In all cases, we again set the root mean square average rf-amplitude to 10 kHz for consistent results. Because some of the published pulse shapes are amplitude-modulated, we obtained slightly different values for calculated durations and bandwidths when considering rf-power compared to the ones reported in [21]. The pulses used were the following ones: composite pulses taken from [5,7,8] for excitation and from [2,5–7,14,45] for inversion; sech/tanh and tanh/tan adiabatic pulses for several bandwidths as described in [46]; BIP [19] and BIBOP [21] inversion pulses, and finally, the pulse shape reported in [44]. As in [21], we numerically determined the maximum bandwidth for which the quality factor Φ reaches 0.98 for all pulses. The results are shown in Fig. 7: none of the reported excitation or inversion pulses reaches the performance of the power-BEBOP/power-BIBOP pulses. Power-BEBOP pulses allow the excitation of a given bandwidth in a much shorter time than any of the other pulses (Fig. 7A and B). For inversion, the gain in pulse performance is less pronounced, with only slight improvements compared to BIBOP pulses. One pulse, the power-optimized inversion pulse reported in [44], can cover the bandwidth of a corresponding BIBOP pulse at a shorter pulse length and almost reaches the performance of the power-BIBOP pulses (Fig. 7C). However, its performance breaks down as soon as variations in rf-amplitude of ϑ = ±20% are considered (Fig. 7D).

4. Discussion

Next to available rf-amplitudes, the applied rf-power poses severe restrictions to many applications in the field of liquid state

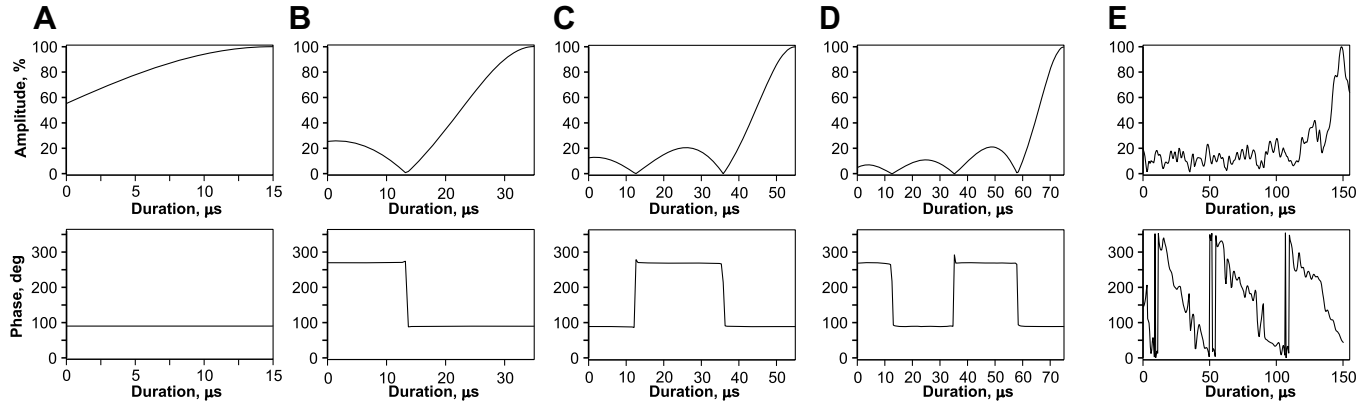

Fig. 3. Amplitude and phase for selected optimized excitation pulses of various durations with limited power deposition found in the optimization for a bandwidth of 30 kHz and ±10% scaling of rf-amplitudes. Pulses similar to polychromatic and ICEBERG pulses [18,41] were found in most optimizations. A common feature of all rf-power optimized excitation pulses is a maximum of the amplitude close to the end of the shape.

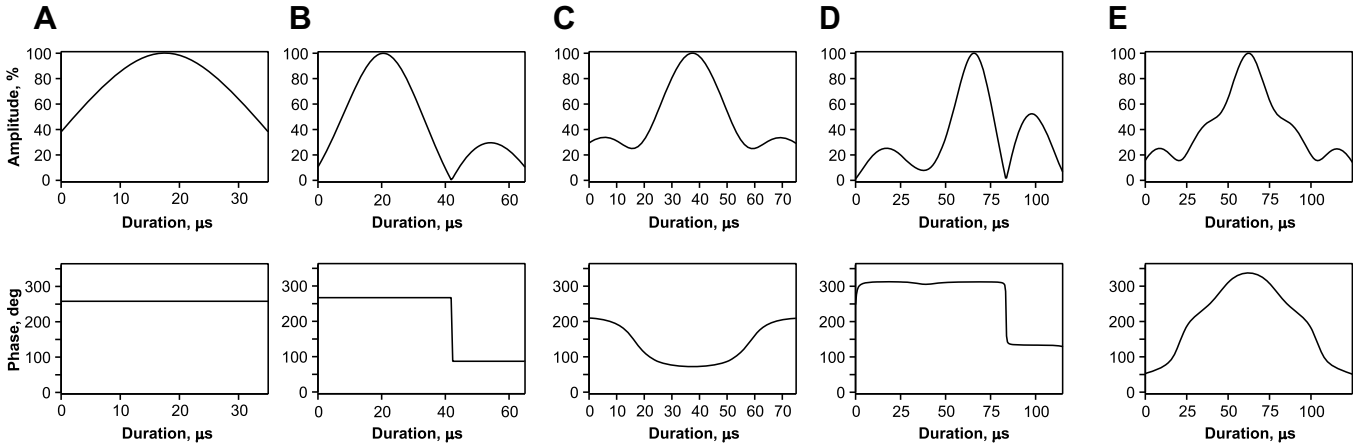

Fig. 4. Amplitude and phase for selected optimized inversion pulses of various durations with limited power deposition found for an optimization bandwidth of 30 kHz and ±10% scaling of rf-amplitudes. Two major pulse families are observed: phase-alternated, amplitude-modulated pulses (A, B, and D) reminiscent of known selective inversion pulses [12,42,43] and pulses with smooth adiabatic-like phases and maximum amplitude at the center of the phase sweep (C and E).

NMR, magnetic resonance imaging and even solid state NMR of biomolecules. The systematic study of rf-power-restricted pulses presented here establishes a set of standards for achievable performance in such applications.

Power-BEBOP and power-BIBOP pulses are, of course, scalable in the same way as conventional pulses. A pulse applied with twice the rf-amplitude (and four times the rf-power) will have half the duration and cover twice the bandwidth of the original pulse with the same robustness with respect to relative variations of the rf-amplitude. This way, the pulses optimized here might be directly transferred to specific applications without even the need of further optimization work.

The power-BEBOP and power-BIBOP pulses described here are optimized with respect to the average rf-power $\overline{P}$, which allows a direct comparison with previously studied amplitude-modulated pulses [21]. In real applications usually the average rf-power of a pulse sequence, including all pulses and delays, has to be minimized. This is, of course, beyond the scope of this article. However, if a pulse sequence or a building block within a pulse sequence consists mainly of excitation and/or inversion pulses, the results of the optimizations shown here give an estimate for the achievable pulse shapes with respect to pulse length, bandwidth, tolerance to rf-amplitude variations and pulse performance. Figs. 1 and 2 can best be used if one or more of the pulse parameters are predefined by the desired experiment and the other parameters are then derived for an optimal solution.

There are also cases where not the average rf-power is the limiting factor for excitation and inversion pulses but the overall energy applied to the sample. Since practically all presented pulse shapes reach the rf-power limit, the total energy of the pulses in Hz is given by $E_{\mathrm{tot}} = \overline{P} \cdot t_{\mathrm{p}} \approx P_{\max} \cdot t_{\mathrm{p}}$. Using this relation and the linear scaling of pulses in general, it is possible to derive a plot correlating the total energy with e.g. the pulse length for a given bandwidth, tolerance to rf-inhomogeneity and pulse performance. An example is shown in Fig. 8 for pulse performances with a cost Φ higher than 0.995 and several bandwidths and values for ϑ. Remarkably, longer power-BEBOP and power-BIBOP pulses do not only lead to lower average rf-power, but apparently also to lower total energies. Unfortunately, the few data points available do not allow to make conclusions on whether there is a minimum energy at a certain pulse length or if E_{tot} can always be reduced by a longer pulse. This issue might be subject to future studies.

Limitations to the applicability of power-BEBOP and power-BIBOP pulses are identical to most excitation and inversion pulses. All pulses are optimized starting with initial $\pm\mathbf{M}_z$ magnetization. The pulse is not defined for any other starting magnetization. So, if a power-BEBOP pulse is required to transfer $\mathbf{M}_x$ magnetization to $\mathbf{M}_z$, the time reversed and 180° phase-shifted pulse shape has

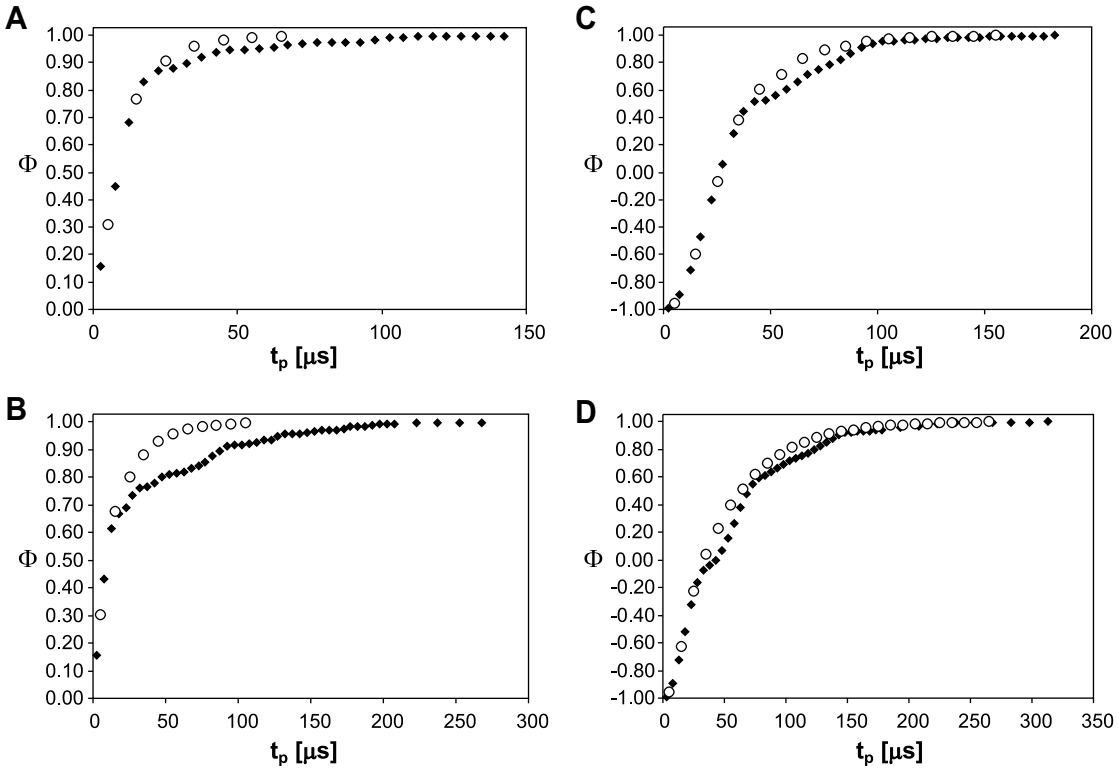

Fig. 5. Comparison of maximum quality factors of rf-power-limited pulses (circles) with quality factors of pulses optimized with limited rf-amplitude (filled diamonds) [21] for excitation (A and B) and inversion (C and D) pulses and offset ranges of 20 kHz (A and C) and 40 kHz (B and D).

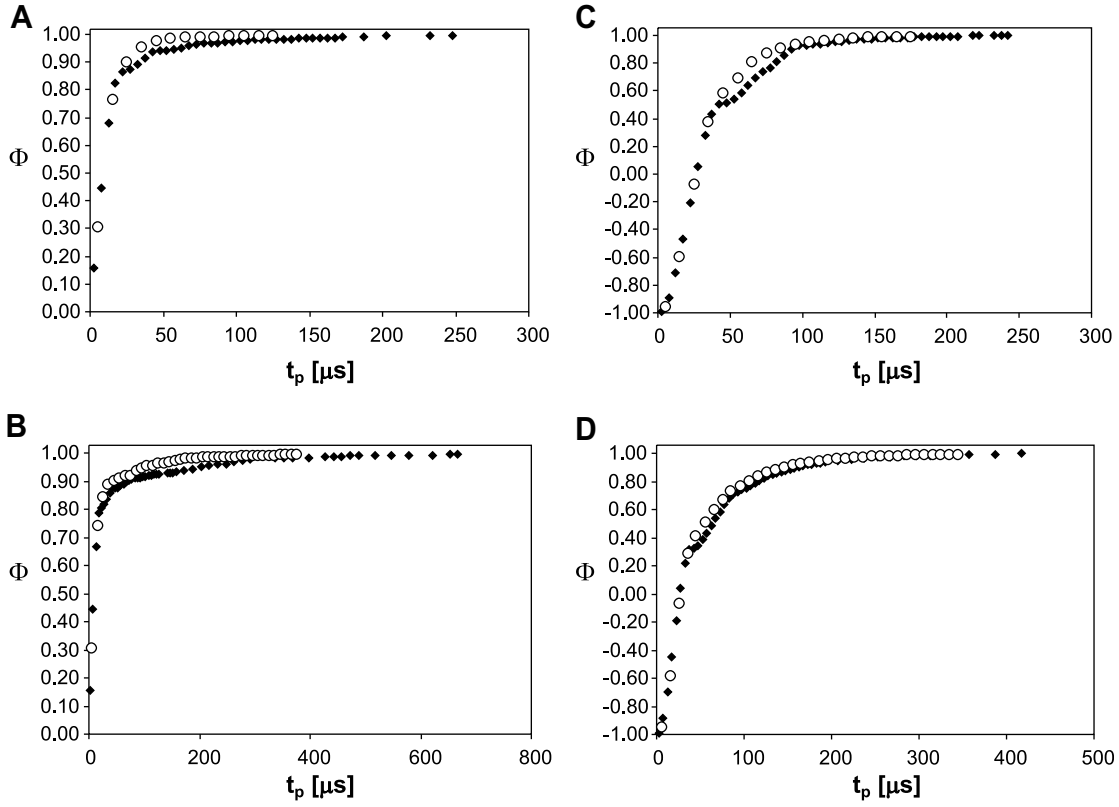

Fig. 6. Comparison of maximum quality factors of rf-power-limited pulses (circles) with quality factors of pulses optimized with limited rf-amplitude (filled diamonds) [21] for excitation (A and B) and inversion (C and D) pulses for a bandwidth of 20 kHz and rf-inhomogeneity ranges of ±10% (A and C) and ±40% (B and D).

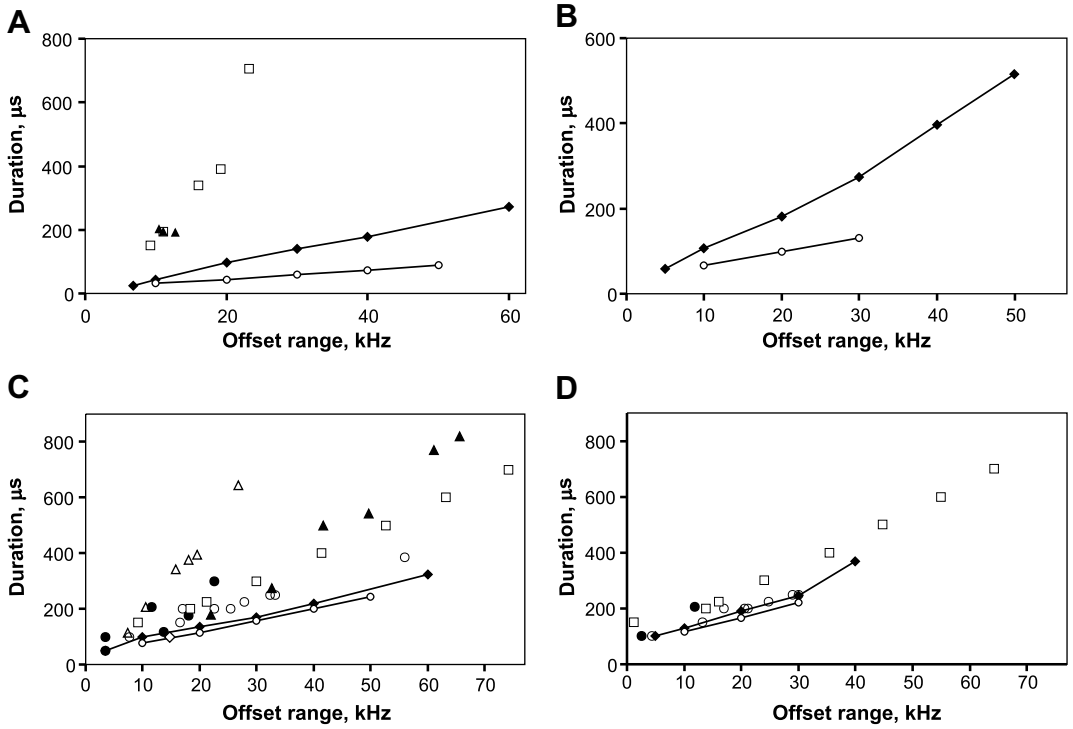

Fig. 7. Comparison of the maximum bandwidths with a quality factor Φ of 0.98 for previously reported broadband excitation (A and B) and inversion pulses (C and D) relative to power-BEBOP and power-BIBOP pulses obtained here. BEBOP and BIBOP pulses [21] are indicated by filled diamonds which are connected by solid lines and power-BEBOP and power-BIBOP pulses are indicated by open circles connected by solid lines, respectively. (A) For excitation, BEBOP pulses were compared with pulses from [7] (squares) and other pulses cited in [47] from original references [5,8] (filled triangles). (B) By taking a rf-variation of ±20% into account, none of the previously known composite pulses reached a quality factor of 0.98. (C) Inversion pulses compared to BIBOP were taken from [44] (open diamond), [45] (filled triangles), [7] (open triangles), [19] (open circles), [46] (open squares), and other inversion pulses cited in [47] from original references [2,5,6,14]. Only the pulse reported in [44] is close to the performance of power-BIBOP pulses. (D) The same comparison including ±20% rf-variation.

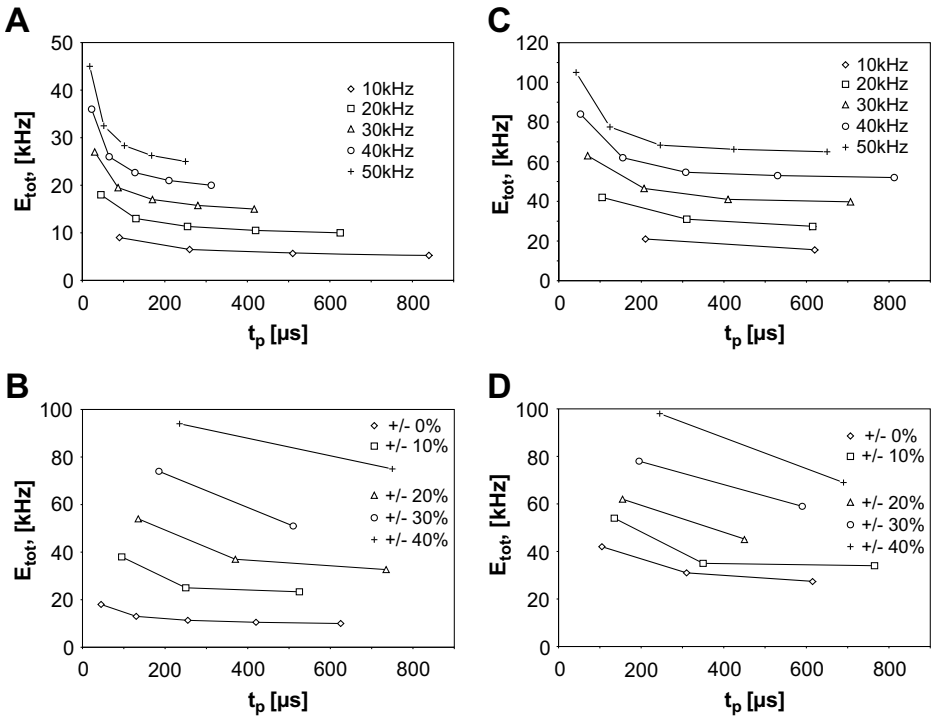

Fig. 8. Total energy $E_{tot} = \overline{P} \cdot t_p$ of power-BEBOP (A and B) and power-BIBOP (C and D) pulses with respect to the pulse length t_p. Pulses used for the plot are the best available pulses from Figs. 1 and 2 with $\Phi > 0.995$ scaled to accommodate the corresponding bandwidths. (A and C) Total energy vs. pulse length for various bandwidths without considering rf-variations. (B and D) The same plots for a constant bandwidth of 20 kHz and various tolerances to B_1-field miscalibrations expressed in ϑ values.

to be used. Also, power-BEBOP and power-BIBOP pulses do not result in uniform unitary rotations. Initial magnetization components different from $\mathbf{M}_z$ will not be transformed in the same way as for a hard 90° or 180° pulse. Power-BIBOP pulses therefore cannot be used as refocussing pulses. Refocussing can, however, be achieved by the application of two consecutive power-BEBOP pulses, following the construction principle described in [48].

Most pulse shapes shown here have smooth amplitude and phase changes and can be implemented on most modern NMR spectrometers. An exception is, for example, the pulse shown in Fig. 3E with significant jumps. Older instruments might not be able to cope with these abrupt phase changes adequately and result in poor pulse performance. Since all rf-power-optimized pulses are amplitude-modulated, amplifier linearity is a must for their correct implementation or pulse shapes have to be adjusted to the specific characteristic of a given spectrometer. The performance with Bruker Avance consoles equipped with SGU units for frequency generation is excellent in our hands and experimental offset profiles coincide very well with the theoretically predicted ones. The pulses should be applicable equally well on other state-of-the-art spectrometers.

Power-BEBOP and power-BIBOP pulses derived are purely rf-power-limited and BEBOP/BIBOP pulses described previously [21] are purely rf-amplitude limited. In reality, both limitations might apply and neither of the pulse families results in optimal performance. However, if appropriate applications arise, the optimization procedure can easily be modified to include both restrictions and optimal pulses should be obtainable within minutes. The performance of such pulses should lie in between the performance of corresponding BEBOP/BIBOP and power-BEBOP/power-BIBOP pulses.

Besides practical aspects on the application of pulses, some theoretical aspects of the work presented should be noted. Interestingly, power-BEBOP pulses with $\vartheta = 0$ have about half the pulse length as corresponding power-BIBOP pulses. This is in contrast to the rf-amplitude-limited pulses, where BEBOP pulses are even slightly longer than corresponding BIBOP pulses at larger bandwidth. It seems as if the large maximum rf-field at the end of power-BEBOP pulse shapes allows a rapid final rotation with uniform phase which otherwise takes a long rf-period to compensate for (see also [29,41], where similar observations have been made for broadband excitation). It is therefore no surprise that power-BEBOP pulse lengths increase significantly as soon as variations in rf-amplitude are considered in the optimizations.

It was already mentioned above that pulse shapes in Fig. 4 partly resemble known selective inversion pulses. Actually, all power-BIBOP pulses that we randomly selected showed a quite high selectivity profile considering their short overall pulse length (data not shown). It seems to be a feature of the optimization process in the case of inversion that the outcoming pulse shapes do automatically fulfill the condition of frequency band-selectivity. For power-BEBOP pulses we do not see such an effect.

5. Conclusion

An algorithm based on optimal control theory has been used to explore the physical limits of rf-power-limited excitation and inversion pulses. With this method, a roughly exponential relation between pulse length and pulse error compensation could be established, and several pulse families for optimal performance have been identified, including constant phase, amplitude-modulated pulses and amplitude-modulated pulses with frequency sweeps similar to previously reported inversion pulses [19,21,44]. A comparison with rf-amplitude-limited pulses and correlations of the minimum pulse length required with respect to excitation/inversion bandwidth and compensation for B_1-field inhomogeneity are given. The pulses will be made available for download on the website http://org.chemie.tu-muenchen.de/people/bulu.

Acknowledgments

N.K. acknowledge Darpa Grant F49620-0101-00556. T.E.S. acknowledges support from NSF Grant CHE-0518174. B.L. thanks the Fonds der Chemischen Industrie and the DFG for financial support (Heisenberg fellowship LU 835/2). S.J.G.'s work was supported by the European integrated programs Bio-DNP and QAP, the DFG (Gl 203/6-1), the SFB 631 and by the Fonds der Chemischen Industrie. We also thank referee #1 for helpful comments which lead to Fig. 8.

References

[1] M.H. Levitt, Symmetrical composite pulse sequences for NMR population inversion: I. Compensation of radiofrequency field inhomogeneity, J. Magn. Reson. 48 (1982) 234–264.
[2] A.J. Shaka, R. Freeman, Composite pulses with dual compensation, J. Magn. Reson. 55 (1983) 487–493.
[3] W.S. Warren, Effects of arbitrary laser of NMR pulse shapes on population-inversion and coherence, J. Chem. Phys. 81 (1984) 5437–5448.
[4] R. Tycko, H.M. Cho, E. Schneider, A. Pines, Composite pulses without phase distortion, J. Magn. Reson. 61 (1986) 90–101.
[5] M.H. Levitt, Composite pulses, Prog. NMR Spectrosc. 18 (1986) 61–122.
[6] D.J. Lurie, Numerical design of composite radiofrequency pulses, J. Magn. Reson. 70 (1986) 11–20.
[7] A.J. Shaka, A. Pines, Symmetric phase-alternating composite pulses, J. Magn. Reson. 71 (1987) 495–503.
[8] R. Freeman, J. Friedrich, X.-L. Wu, A pulse for all seasons—Fourier-transform spectra without a phase gradient, J. Magn. Reson. 79 (1988) 561–567.
[9] D.B. Zax, G. Goelman, S. Vega, Amplitude modulated composite pulses, J. Magn. Reson. 80 (1988) 375–382.
[10] J.M. Böhlen, M. Rey, G. Bodenhausen, Refocusing with chirped pulses for broadband excitation without phase dispersion, J. Magn. Reson. 84 (1989) 191–197.
[11] L. Emsley, G. Bodenhausen, Gaussian pulse cascades—new analytical functions for rectangular selective inversion and in-phase excitation in NMR, Chem. Phys. Lett. 165 (1990) 469–476.
[12] B. Ewing, S.J. Glaser, G.P. Drobny, Development and optimization of shaped NMR pulses for the study of coupled spin systems, Chem. Phys. 147 (1990) 121–129.
[13] M. Garwood, Y. Ke, Symmetric pulses to induce arbitrary flip angles with compensation for rf inhomogeneity and resonance offsets, J. Magn. Reson. 94 (1991) 511–525.
[14] M.A. Keniry, B.C. Sanctuary, Experimental verification of composite inversion pulses obtained by series expansion of the offset angle, J. Magn. Reson. 97 (1992) 382–384.
[15] D. Abramovich, S. Vega, Derivation of broadband and narrowband excitation pulses using the Floquet formalism, J. Magn. Reson. A 105 (1993) 30–48.
[16] J.M. Böhlen, G. Bodenhausen, Experimental aspects of chirp NMR spectroscopy, J. Magn. Reson. A 102 (1993) 293–301.
[17] V.L. Ermakov, G. Bodenhausen, Broadband excitation in magnetic resonance by self-refocusing doubly frequency-modulated pulses, Chem. Phys. Lett. 204 (1993) 375–380.
[18] É. Kupče, R. Freeman, Wideband excitation with polychromatic pulses, J. Magn. Reson. A 108 (1994) 268–273.
[19] M.A. Smith, H. Hu, A.J. Shaka, Improved broadband inversion performance for NMR in liquids, J. Magn. Reson. 151 (2001) 269–283.
[20] K.E. Cano, M.A. Smith, A.J. Shaka, Adjustable, broadband, selective excitation with uniform phase, J. Magn. Reson. 155 (2002) 131–139.
[21] K. Kobzar, T.E. Skinner, N. Khaneja, S.J. Glaser, B. Luy, Exploring the limits of broadband excitation and inversion, J. Magn. Reson. 170 (2004) 236–243.
[22] S. Conolly, D. Nishimura, A. Macovski, Optimal control to the magnetic resonance selective excitation problem, IEEE Trans. Med. Imaging MI-5 (1986) 106–115.
[23] J. Mao, T.H. Mareci, K.N. Scott, E.R. Andrew, Selective inversion radiofrequency pulses by optimal control, J. Magn. Reson. 70 (1986) 310–318.
[24] D. Rosenfeld, Y. Zur, Design of adiabatic selective pulses using optimal control theory, Magn. Reson. Med. 36 (1996) 401–409.
[25] T.E. Skinner, T.O. Reiss, B. Luy, N. Khaneja, S.J. Glaser, Application of optimal control theory to the design of broadband excitation pulses for high resolution NMR, J. Magn. Reson. 163 (2003) 8–15.
[26] T.E. Skinner, T.O. Reiss, B. Luy, N. Khaneja, S.J. Glaser, Reducing the duration of broadband excitation pulses using optimal control with limited RF amplitude, J. Magn. Reson. 167 (2004) 68–74.

[27] T. Skinner, T.O. Reiss, B. Luy, N. Khaneja, S.J. Glaser, Tailoring the optimal control cost function to enable shorter broadband excitation pulses, J. Magn. Reson. 172 (2005) 17–23.
[28] T.E. Skinner, K. Kobzar, B. Luy, R. Bendall, W. Bermel, N. Khaneja, S.J. Glaser, Optimal control design of constant amplitude phase-modulated pulses: application to calibration-free broadband excitation, J. Magn. Reson. 179 (2006) 241–249.
[29] N.I. Gershenzon, K. Kobzar, B. Luy, S.J. Glaser, T.E. Skinner, Optimal control design of excitation pulses that accommodate relaxation, J. Magn. Reson. 188 (2007) 330–336.
[30] K. Kobzar, B. Luy, N. Khaneja, S.J. Glaser, Pattern pulses: design of arbitrary excitation profiles as a function of pulse amplitude and offset, J. Magn. Reson. 173 (2005) 229–235.
[31] N. Khaneja, S.J. Glaser, R. Brockett, Sub-Riemannian geometry and time optimal control of three spin systems: quantum gates and coherence transfer, Phys. Rev. A 65 (2002) 032301.
[32] T.O. Reiss, N. Khaneja, S.J. Glaser, Time-optimal coherence-order-selective transfer of in-phase coherence in heteronuclear IS spin systems, J. Magn. Reson. 154 (2002) 192–195.
[33] N. Khaneja, S.J. Glaser, Efficient transfer of coherence through Ising spin chains, Phys. Rev. A 66 (2002) 060301(R).
[34] T.O. Reiss, N. Khaneja, S.J. Glaser, Broadband geodesic pulses for three spin systems: time-optimal realization of effective trilinear coupling terms and indirect SWAP gates, J. Magn. Reson. 165 (2003) 95–101.
[35] N. Khaneja, T.O. Reiss, B. Luy, S.J. Glaser, Optimal control of spin dynamics in the presence of relaxation, J. Magn. Reson. 162 (2003) 311–319.
[36] N. Khaneja, B. Luy, S.J. Glaser, Boundary of quantum evolution under decoherence, Proc. Natl. Acad. Sci. USA 100 (2003) 13162–13166.
[37] D. Stefanatos, N. Khaneja, S.J. Glaser, Optimal control of coupled spins in presence of longitudinal relaxation, Phys. Rev. A 69 (2004) 022319.
[38] C.T. Kehlet, Design of optimum liquid-state NMR experiments in the presence of relaxation, Master Thesis, München, 2003.
[39] T.O. Reiss, Anwendung der Steuerungstheorie auf die kernmagnetische Resonanzspektroskopie—von der Entwicklung computergestützter Optimierungsmethoden bis zur experimentellen Umsetzung, Ph.D. Thesis, München, 2002.
[40] N. Khaneja, T.O. Reiss, C. Kehlet, T. Schulte-Herbrüggen, S.J. Glaser, Optimal control of coupled spin dynamics: design of NMR pulse sequences by gradient ascent algorithm, J. Magn. Reson. 172 (2005) 296–305.
[41] N.I. Gershenzon, T.E. Skinner, M. Nimbalkar, B. Luy, B. Brutscher, N. Khaneja, S.J. Glaser, Linear phase slope in pulse design: application to coherence transfer, J. Magn. Reson. 192 (2008) 235–243.
[42] C. Bauer, R. Freeman, T. Frenkiel, J. Keeler, A.J. Shaka, Gaussian pulses, J. Magn. Reson. 58 (1984) 442–457.
[43] L. Emsley, G. Bodenhausen, Gaussian pulse cascades: new analytical functions for rectangular selective inversion and in-phase excitation in NMR, Chem. Phys. Lett. 165 (1990) 469–476.
[44] P.B. Barker, X. Golay, D. Artemov, R. Ouwerkerk, M.A. Smith, A.J. Shaka, Broadband proton decoupling for in vivo brain spectroscopy in humans, Magn. Reson. Med. 45 (2001) 226–232.
[45] A.J. Shaka, Composite pulses for ultra-broadband spin inversion, Chem. Phys. Lett. 120 (1985) 201–205.
[46] Y.A. Tesiram, M.R. Bendall, Universal equations for linear adiabatic pulses and characterization of partial adiabaticity, J. Magn. Reson. 156 (2002) 1–15.
[47] W.E. Hull, Experimental aspects of two-dimensional NMR, in: W.R. Croasmun, R.M.K. Carlson (Eds.), Two-Dimensional NMR Spectroscopy—Applications for Chemists and Biochemists, VCH Publishers, New York, 1994, pp. 67–456.
[48] B. Luy, K. Kobzar, T.E. Skinner, N. Khaneja, S.J. Glaser, Construction of universal rotations from point to point transformations, J. Magn. Reson. 176 (2005) 179–186.